The role of an evolutionarily conserved *cis*-proline in the thioredoxin-like domain of human class Alpha glutathione transferase A1-1

Chris NATHANIEL*, Louise A. WALLACE†, Jonathan BURKE* and Heini W. DIRR*[1]

*Protein Structure-Function Research Programme, School of Molecular and Cell Biology, University of the Witwatersrand, Johannesburg 2050, South Africa, and †Department of Biochemistry and Molecular Pharmacology, University of Massachusetts Medical School, Worcester, MA 01605, U.S.A.

The thioredoxin-like fold has a $\beta\alpha\beta\alpha\beta\beta\alpha$ topology, and most proteins/domains with this fold have a topologically conserved *cis*-proline residue at the N-terminus of β-strand 3. This residue plays an important role in the catalytic function and stability of thioredoxin-like proteins, but is reported not to contribute towards the stability of glutathione S-transferases (GSTs) [Allocati, Casalone, Masulli, Caccarelli, Carletti, Parker and Di Ilio (1999) FEBS Lett. **445**, 347–350]. In order to further address the role of the *cis*-proline in the structure, function and stability of GSTs, *cis*-Pro-56 in human GST (hGST) A1-1 was replaced with a glycine, and the properties of the P56G mutant were compared with those of the wild-type protein. Not only was the catalytic function of the mutant dramatically reduced, so was its conformational stability, as indicated by equilibrium unfolding and unfolding kinetics experiments with urea as denaturant. These findings are discussed in the context of other thioredoxin-like proteins.

Key words: conformational stability, glutathione, thioredoxin fold.

INTRODUCTION

The thioredoxin fold is a versatile scaffold found in many protein families with diverse functions. The fold has been identified in the three-dimensional structures of at least 12 protein families despite their low sequence identities: thioltransferases (includes thioredoxins and small glutaredoxins), protein disulphide isomerase-like, calsequestrin, disulphide-bond formation facilitator DsbA, N-terminal domain of glutathione S-transferases (GSTs), phosducin, N-terminal domain of endoplasmic reticulum protein ERP29, spliceosomal protein U5-15kD, C-terminal domain of disulphide-bond isomerase DsbC, glutathione peroxidase-like, thioredoxin-like 2Fe-2S ferredoxin and arsenate reductase ArsC (see http://scop.mrc-lmb.cam.ac.uk/scop/data/scop.b.d.fe.b.html). The thioredoxin fold is characterized by a $\beta\alpha\beta\alpha\beta\beta\alpha$ topology with the β-sheet sandwiched between two layers of α-helices [see Figure 1 for the thioredoxin-like fold in human class Alpha GST with two type-1 subunits (hGST A1-1)]. Structure-based sequence alignments with thioredoxin show that a *cis*-proline at the N-terminus of β-strand 3 is conserved in most members of the superfamily. It is not observed in the structures of the spliceosomal protein U5-15kD and seven of the 10 members of the glutathione peroxidase-like family.

The cystolic GSTs, a large thioredoxin-like family, are multifunctional proteins that can be grouped into at least 12 classes: Alpha, Beta, Delta, Mu, Phi, Pi, Theta, Kappa, Sigma, Tau, Omega and Zeta (for a review, see [1]). Recently, glutaredoxin-2 [2], Ure2p [3] and Clic1 (chloride intracellular channel) protein [4] have also been classified as members of the GST structural family. The *cis*-proline is conserved in the thioredoxin-like N-terminal domain of all the members of this family, and its *cis–trans* isomerization contributes to the folding kinetics of hGST A1-1 [5]. The active site of the GSTs can be divided into two adjacent subsites: the G-site for binding GSH and the H-site for binding hydrophobic electrophilic substrates [6]. The G-site is formed primarily by the thioredoxin-like N-terminal domain, whereas the C-terminal domain forms the H-site. The conserved *cis*-proline is located at the G-site where it facilitates the backbone to assume the correct conformation for the formation of two hydrogen bonds between the main chain of the protein and the cysteinyl moiety of GSH [7].

The role of the conserved *cis*-proline in the function and stability of thioredoxin-like proteins has been investigated for *Escherichia coli* thioredoxin [8], DsbA [9], rat GST A1-1 [10] and *Proteus mirabilis* GST B1-1 [11]. These studies indicate the importance of the residue in catalytic function. Proline-to-alanine mutations are also shown to reduce the conformational stability of thioredoxin [8] and DsbA [9], whereas the corresponding mutation in GST B1-1 is reported not to impact on the protein's stability and unfolding/refolding kinetics [11]. A thermal-inactivation study with rat GST A1-1 suggested that the *cis*-proline is important for maintaining the proper conformation of the protein [10]. In order to further address the role of the *cis*-proline in the structure, function and stability of GSTs, *cis*-Pro-56 in hGST A1-1 was replaced with a glycine, and the properties of the P56G mutant were compared with those of the wild-type protein. Not only was the catalytic function of the mutant dramatically reduced, so was its conformational stability, as indicated by equilibrium unfolding and unfolding kinetics experiments with urea as a denaturant.

EXPERIMENTAL

Materials

The plasmid pKHA1 that encodes hGST A1-1 was a gift from Professor B. Mannervik (Uppsala University, Uppsala, Sweden) [12]. The P56G mutant was generated using the ExSite™ PCR-based site-directed mutagenesis kit (Stratagene). The CCA codon for Pro-56 was altered to a glycine codon (GGA), and a translationally silent mutation, coding

Abbreviations used: ANS, 8-anilinonaphthalene-1-sulphonate; CDNB, 1-chloro-2,4-dinitrobenzene; GST, glutathione S-transferase; hGST A1-1, human class Alpha GST with two type-1 subunits.

[1] To whom correspondence should be addressed (e-mail 089dirr@cosmos.wits.ac.za).

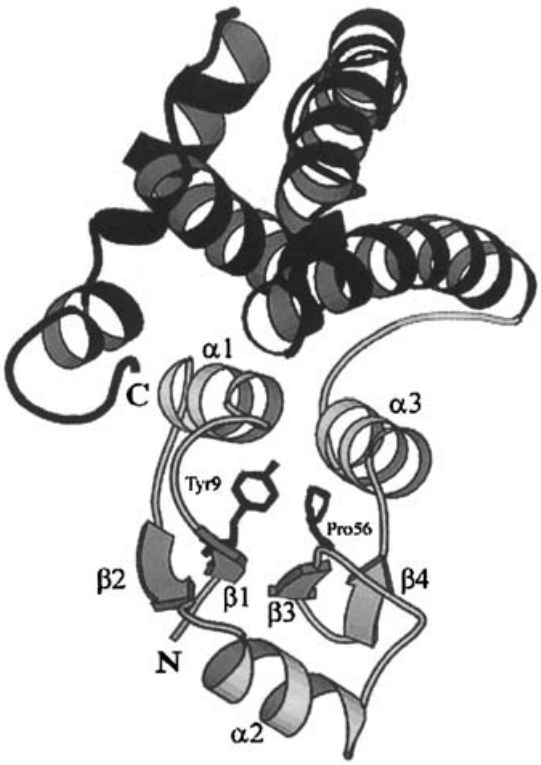

Figure 1 Ribbon representation showing one subunit of the homodimeric hGST A1-1

The thioredoxin-like N-domain is shown in a lighter shade. The side chains of the topologically conserved Pro-56 and the catalytically important Tyr-9 are indicated. The diagram was generated by the programme MOLSCRIPT [31] using the PDB file 1gse.

for the diagnostic *Eco*RV restriction site, was engineered into the plasmid. The mutations were introduced directly into the pKHA1 plasmid using the following primers: P56GFP (5′-AGGGTGAACGACTTTGTAGTAGTCTATAGG-3′) and P56-GRP (5′-*TCC*CACTTGCTGAAACATCATCAGATATCC-3′). In primer P56GRP, the underlined nucleotides represent a translationally silent mutation which incorporated a unique restriction site *Eco*RV for screening of the mutant plasmid, and the italicized nucleotides represent the mutation that generates the Pro-to-Gly substitution (P56G).

The PCR reaction was carried out as detailed in the manufacturer's instruction manual and the PCR product transformed into *Escherichia coli* XL1-Blue supercompetent cells. DNA sequencing was done using an ABI Prism 310 Genetic Analyser from PE Biosystems (Foster City, CA, U.S.A.) to confirm the mutations and that no other mutations were present. Wild-type and mutant enzymes were purified by ion-exchange chromatography on a CM-Sepharose column [13]. The purity and molecular mass of the protein were assessed by SDS/PAGE [14] and size-exclusion chromatography HPLC. Protein concentrations were determined using a molar absorption coefficient of $38200\ M^{-1} \cdot cm^{-1}$ as calculated by the method described in [15].

Steady-state enzyme kinetics

The catalytic activity of the P56G mutant was determined spectrophotometrically at 340 nm according to the method of [16] using an absorption coefficient of $9600\ M^{-1} \cdot cm^{-1}$ for the formation of 1-(*S*-glutathionyl)-2,4-dinitrobenzene. Standard assays contained a final concentration of 1 mM GSH, 1 mM 1-chloro-2,4-dinitrobenzene (CDNB) and 3 % (v/v) ethanol. Reactions were followed for 60 s at 21 °C, which yielded linear progress curves. All reactions were corrected for non-enzymic rates.

The K_m for GSH was determined by varying the concentration of GSH (1–150 mM), keeping CDNB constant at 2 mM. In the same way, the K_m for CDNB was determined using 0.1–2 mM CDNB and 20 mM GSH. Data were fitted to a single rectangular hyperbolic curve and the kinetic parameters determined using the Michealis–Menten equation. The catalytic efficiency (k_{cat}/K_m) for CDNB was determined at low CDNB concentrations (0.05–0.15 mM) and 20 mM GSH, and calculated from the slope of linear plots of velocity versus CDNB concentration for three different protein concentrations. All rates were corrected for non-enzymic reactions.

Spectroscopic measurements

Protein samples (1 μM) were excited at 295 nm for measuring tryptophan fluorescence spectra in a Hitachi model 850 fluorescence spectrofluorimeter. The excitation and emission bandwidths were set at 5 nm. The binding of the amphipathic dye 8-anilinonaphthalene-1-sulphonate (ANS) to protein was monitored using enhanced fluorescence of the dye when excited at 390 nm. Far-UV CD spectra (250–200 nm) were measured with protein at a concentration of 2 μM in a Jasco J-810 spectrapolarimeter with a 2 mm pathlength and averaged over 20 runs.

Binding studies

The binding of various ligands (glutathione, glutathione sulphonate and *p*-bromobenzyl glutathione) to the wild-type and P56G mutant proteins was measured by tryptophan fluorescence quenching. Samples of 1 μM protein in 20 mM sodium phosphate, pH 6.5, 0.1 M NaCl, 1 mM EDTA and 0.02 % sodium azide were titrated with increasing concentrations of ligand and the emission was monitored at 325 nm (excitation wavelength was set at 295 nm). Data were corrected for buffer controls and dilution.

Acrylamide quenching

Quenching of the intrinsic fluorescence of Trp-20 in the wild-type and P56G mutant proteins (1 μM) by acrylamide (0–0.3 M) was measured as described previously [17]. The data were analysed according to the Stern–Volmer equation $F_o/F = 1 + K_{SV}[Q]$, where F_o is the tryptophan fluorescence in the absence of acrylamide, F is the tryptophan fluorescence in the presence of increasing concentrations of added quenching agent Q, and K_{SV} is the Stern–Volmer quenching constant.

Unfolding/stability studies

All equilibrium unfolding and reversibility studies were performed at 20 °C in 20 mM sodium phosphate buffer, pH 6.5, containing 1 mM EDTA and 0.02 % sodium azide. The reversibility of unfolding was determined as described [18]. Protein samples (1 μM) were incubated with urea (0–8 M) for 1 h to achieve equilibrium prior to measurements. Tryptophan fluorescence and CD ellipticity at 222 nm were used as structural

probes to obtain unfolding curves. The fluorophore, Trp-20, was selectively excited at 295 nm and its emission intensity monitored at 325 nm (for folded protein) and at 355 nm (for unfolded protein). Rayleigh scattering (due to aggregation) was assessed using excitation and emission wavelengths set at 295 nm. The unfolding curves were analysed according to the two-state assumption as described in [19] to obtain the unfolding parameters $\Delta G(H_2O)$, the change in free energy of unfolding in the absence of denaturant, and the *m*-value, the dependence of ΔG on denaturant concentration.

Urea-induced unfolding kinetics of the P56G mutant (1 μM) were monitored by tryptophan fluorescence in an Applied PhotoPhysics SX-18MV stopped-flow mixing device and the data analysed as described previously [18].

Table 1 Kinetic and dissociation constants for wild-type and P56G hGST A1-1

Kinetic parameter	Wild-type A1-1	P56G mutant
Specific activity (μmol/min per mg)	44.6 ± 2.3	0.84 ± 0.65
K_m^{GSH} (mM)	0.52 ± 0.4	21.9 ± 2.0
K_m^{CDNB} (mM)	0.33 ± 0.06	1.85 ± 0.15
k_{cat}/K_m^{CDNB} (mM/s)	103.5 ± 28.3	41.5 ± 3.7
Binding affinity (K_d)		
GSH (mM)	0.2 ± 0.05	3.98 ± 1.18
GSH sulphonate (μM)	1.55 ± 0.36	17.41 ± 2.52
p-Bromobenzyl GSH (μM)	4.93 ± 1.17	10.67 ± 0.35

RESULTS

Properties of the P56G hGST A1-1 mutant

Like the wild-type protein, the P56G hGST A1-1 mutant is dimeric with a molecular mass of about 55 kDa. The fluorescence and far-UV CD spectra for the P56G mutant are similar to those for the wild-type protein, indicating that the mutation had not induced any major structural changes. The catalytic function of hGST A1-1, however, was severely compromised by replacing Pro-56 with a glycine, and the mutant exhibited less than 2 % of the activity of the wild-type enzyme (Table 1). The P56G mutation increased the K_m for GSH about 17-fold and for CDNB about 5-fold, whereas the catalytic efficiency (k_{cat}/K_m) towards CDNB was decreased about 3-fold. Binding affinities for various ligands are also shown in Table 1. Compared with the wild type, the P56G mutant binds the G-site ligands GSH and its sulphonate analogue much more weakly than the product analogue *p*-bromobenzyl GSH, which binds both the G-site and H-site. The fluorescence spectra of the amphipathic dye ANS bound to protein were similar for both wild-type and mutant enzymes, with an emission maximum at 485 nm. Furthermore, the exposure of the lone tryptophan (Trp-20) to solvent was assessed by acrylamide quenching to be similar for both wild-type ($K_{SV} = 2.1\ M^{-1}$ [13]) and P56G mutant ($K_{SV} = 2.8\ M^{-1}$) proteins.

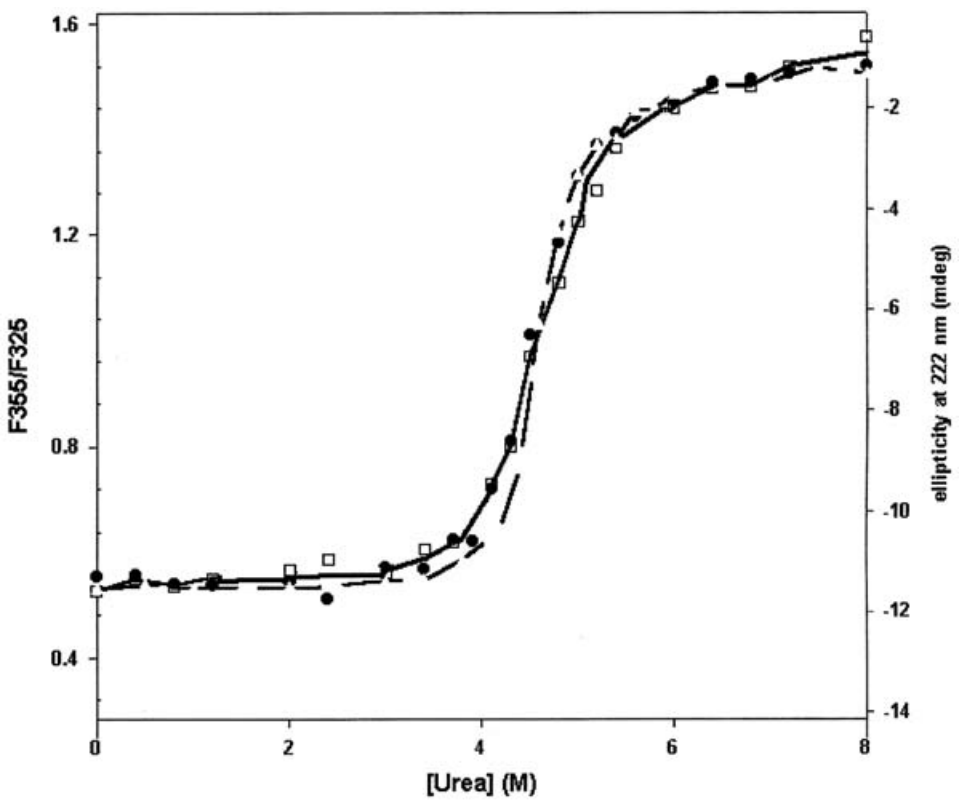

Figure 2 Unfolding curves of P56G mutant hGST A1-1

Structural changes were monitored by tryptophan fluorescence (●) and ellipticity at 222 nm (□). The ratio of F355/F325 represents the fluorescence of the unfolded and folded proteins respectively. The continuous line represents the fitted curve of the mutant. The broken line represents the curve for wild-type hGST A1-1 [18].

Table 2 Equilibrium unfolding parameters for P56G mutant and wild-type proteins

$\Delta G(H_2O)$ is the change in free energy of unfolding in the absence of denaturant; *m*-value is the dependence of ΔG on denaturant concentration; C_m is the value of the midpoint of the urea unfolding transition curve. Data for the wild-type protein are shown for comparison and are taken from [13].

	P56G mutant	Wild-type A1-1 [13]
$\Delta G(H_2O)$ (kJ/mol)	89.5 ± 2.1	115.1
m-value (kJ/mol per M urea)	12.6 ± 0.4	17.6
C_m (M)	4.6 ± 0.1	4.6

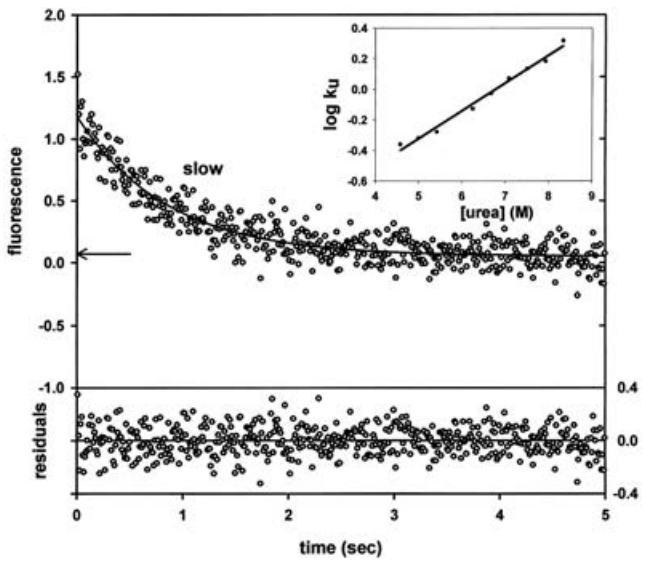

Figure 3 Unfolding kinetics trace for monitored fluorescence of hGST A1-1 P56G mutant

Excitation was at 280 nm and emission was measured with a 320 nm cut-off filter. Only the slow phase is observed at 8.3 M urea and 25 °C. The fast phase occurs during the dead time of the instrument. The arrow indicates the fluorescence signal for the native folded protein. Inset: the urea dependence of the rate of the slow unfolding phase.

Equilibrium unfolding

Unfolding of the P56G mutant protein was highly reversible with recoveries in excess of 95%. The fluorescence- and CD-unfolding curves for the mutant, shown in Figure 2, are monophasic and coincident, suggesting the simultaneous loss of tertiary and secondary structure as the protein unfolds. Conformational stability data for the wild-type and P56G mutant proteins, derived from the unfolding curves, are reported in Table 2 and indicate that the mutant is less stable than the wild-type by 25.5 kJ/mol. Although both proteins have similar C_m values (the value of the midpoint of the urea unfolding transition curves), the slope of the unfolding transitions for the mutant is shallower than that of the wild type (Figure 2), as indicated by the smaller *m*-value.

Unfolding kinetics

Like the wild-type protein [18], the unfolding kinetics of the P56G mutant displayed two phases (Figure 3): a fast phase with increasing fluorescence intensity and a slow phase with decreasing fluorescence intensity. However, unlike the fast unfolding phase for the wild-type protein, which was observed at 25 °C [18], the corresponding phase for the mutant occurred within the dead time (2 ms) at 25 °C. Only part of the fast phase for the mutant was observed at lower temperature (5 °C; results not shown). The slow unfolding phase for the mutant is best described by a single exponential function (see residuals in Figure 3), with a rate constant of 2.1 s^{-1}. This is about 10-fold faster than the unfolding rate constant for the slow unfolding phase for wild-type hGST A1-1 (0.24 s^{-1}) under identical conditions [18]. The slow phase shows a linear dependence on urea concentration (see inset to Figure 3), yielding a slope (m_u) of 452 J/mol per M urea at 25 °C. The corresponding m_u-value for the wild type is 1130 J/mol per M urea (2.5-fold larger) [18].

DISCUSSION

Structure and function

The replacement of Pro-56 with a glycine did not have any significant impact on the overall structure of hGST A1-1. Since the dimeric structure was preserved, it is unlikely that the conformation of the loop sequence connecting α-helix 2 to β-strand 3, with Gly-56 at its C-terminus, was severely affected by the mutation. This loop, located near the subunit interface, contains a hydrophobic lock-and-key intersubunit motif that is involved in stabilizing class Alpha [13], Pi [20] and Mu [21] GST dimers. Furthermore, the intrasubunit domain–domain interface appeared to be unaffected by the P56G mutation, since the accessibility and spectral properties of Trp-20, a sensitive probe for monitoring changes at the domain interface [22], were unaltered. These findings are consistent with those for the crystal structures of DsbA, in which the corresponding *cis*-proline (Pro-151) in its thioredoxin-like domain was replaced with an alanine [9]. The overall structures of the wild-type and mutant proteins were very similar, except for the backbone conformation from Gly-149 to Ala-152 with Ala-151 assuming a *trans* conformation.

The P56G mutation significantly affected the catalytic functioning of hGST A1-1 with its activity almost completely abolished. The kinetics behaviour of the P56G mutant is consistent with that reported for the P56A mutant of the rat GST A1-1 [10] and the corresponding P53S mutant of a GST from *P. mirabilis* [11], both of which also display diminished catalytic function. The affinity of GSH for these GSTs appears not to be significantly altered by the replacement with either alanine or serine, and the diminished catalytic efficiencies of the mutants are caused mainly by lowered k_{cat} values. Substitutions of the corresponding *cis*-proline in other members of the thioredoxin-like superfamily (P151A DsbA [9] and P73A thioredoxin [8]) also resulted in greatly diminished activities. The impact of the mutation on the enzyme was indicated when the P56G variant bound very weakly to the *S*-hexylglutathione affinity column used in the purification. Kinetics and ligand-binding data suggest that the G-site, to which the thiol substrate glutathione binds, is compromised by the P56G mutation to a much greater extent than the adjacent H-site. In the wild-type protein, the backbone of Val-55, located at the base of the G-site, forms a hydrogen-bonded anti-parallel sheet with the main-chain atoms of the cysteinyl moiety of GSH [23]. Although the structural data for hGST A1-1 indicate no major differences between the wild-type and mutant proteins, the functional data suggest that the conformations of the Val-55–Pro-56 and Val-55–Gly-56 regions are not identical. The weaker binding of GSH and its sulphonate analogue to the G-site of the P56G mutant suggests that this interaction between the protein and substrate backbones is adversely affected. The weaker binding of glutathione is also

reflected in its substantially increased K_m. The smaller effect of the mutation on the binding of *p*-bromobenzyl GSH is most likely due to the binding of its *p*-bromobenzyl moiety to the H-site. The loss of activity of the P151A DsbA mutant is proposed to be a consequence (in part) of a loss of main-chain hydrogen bonding between the protein at Val-150 and the peptide substrate, due to a conformational change in the backbone at Val-150-Ala-151 (see above) [9].

In hGST A1-1, Pro-56 packs against Tyr-9, the catalytically important residue for activating glutathione at the active site [24], Arg-15 (also catalytically important [25]) and Met-16 contacts that could play an important role in maintaining the correct conformation at the G-site. The removal of the pyrrolidine ring of Pro-56 in the P56G mutant would create a small cavity that might disrupt the packing environment in this region. This could result in (i) less efficient thiol substrate binding (due to an altered backbone conformation at Val-55), (ii) an unfavourable orientation between the thiol group of GSH and the hydroxyl group of Tyr-9 and (iii) a change in the hydrogen bonding between the amide nitrogen of Arg-15 and the hydroxyl group of Tyr-9. The latter two could explain the dramatic decrease in k_{cat} for *cis*-proline mutants of GSTs [10,11]. For thioredoxin and DsbA, their *cis*-prolines (Pro-76 and Pro-151, respectively) make van-der-Waals contacts with the active-site redox disulphides [9,26], and their replacement with alanines produces local conformational changes resulting in diminished activities. Altered activity of DsbA is due largely to the reduced oxidizing power of the P151A mutant [9].

Conformational stability

Not only does the P56G mutation affect the catalytic function of hGST A1-1, it also destabilizes the conformation of the protein by about 25 kJ/mol. Similar findings were reported for other members of the thioredoxin-like superfamily; the P76A mutant of thioredoxin is destabilized by 15.9 kJ/mol [8], and the P151A mutant of DsbA destabilized by 23.5–28.3 kJ/mol [9]. It is interesting to note that the replacement of *cis*-Pro-53 with a serine in the *P. mirabilis* GST was reported not to affect the overall stability and unfolding kinetics of the protein [11]. However, the mutant enzyme was found to be more sensitive to thermal inactivation than the wild type. The extent of the decrease in stability of the P56G hGST A1-1 mutant seems too large for a proline-to-alanine substitution alone, suggesting that the mutation introduces a local conformational change in hGST A1-1. A similar scenario exists for the thioredoxin and DsbA proline-to-alanine mutants and which was explained by the introduction of a *trans*-peptide bond rather than a *cis* bond at the site of substitution [8,9]. Although glycine can assume either a *cis* or *trans* conformation, it is not clear which is present at Gly-56 in P56G hGST A1-1.

Unfolding of the wild-type hGST A1-1 is highly co-operative, as indicated by its steep unfolding transition and corresponding *m*-value (17.6 kJ/mol per M urea), the magnitude of which closely agrees with that predicted for the size of the protein (20.1 kJ/mol per M urea) [18]. The unfolding transition of the P56G mutant, however, is less steep, yielding a lower *m*-value (12.6 kJ/mol per M urea), suggesting decreased co-operativity within the structure and possibly the accumulation, at equilibrium, of an unfolding intermediate [27]. The intermediate cannot be highly populated, since the transition occurred in a single step and was independent of the spectroscopic probes used to follow unfolding. Decreased stabilities and co-operativities have also been reported for other mutants of hGST A1-1 [18,28].

Although Pro-56 is not located in the core of the thioredoxin-like domain of hGST A1-1 (and other thioredoxin-like proteins), it is located at the N-terminus of an internal β-strand (β-strand 3) of the $\beta_3\beta_4\alpha_3$ C-subdomain. The N-subdomain consists of $\beta_1\alpha_1\beta_2$ and is connected to the C-subdomain by sequence containing α-helix 2. Studies with the N- and C-subdomains of thioredoxin indicate that the packing and interactions between the neighbouring strands of the subdomains (i.e. β-strand 1 and β-strand 3 in hGST A1-1) are important for maintaining the stability of these subdomains [29]. Given the conservation of the *cis*-proline in most thioredoxin-like proteins, stabilization of their β-sheet in the thioredoxin-like domain may require the *cis* bond. Recently, it was proposed that the thioredoxin-like domain, domain 1, of hGST P1-1 is less stable than domain 2 and that an unfolding intermediate with a partially folded domain 1 and structured domain 2 might exist [30]. In the light of the packing environment about Pro-56 in hGST A1-1 (see above), it is plausible that the β-sheet in the P56G mutant is not as tightly packed as that in the wild-type protein, resulting in a destabilized less co-operative hydrophobic core in domain 1, resulting in a reduced *m*-value.

Unfolding kinetics of the P56G mutant are consistent with diminished stability of the native state of hGST A1-1, since both phases occur much faster than the corresponding phases for the native wild type, with the mutant's fast phase occurring within the dead time (2 ms). The slow phase is the major unfolding event representing the complete dissociation and unfolding of the hGST A1-1 dimer to two unfolded monomers [18]. The linear dependence of the slow unfolding rate on urea concentration for both the P56G mutant (this study) and wild type [18], suggests that no changes occur in the rate-limiting step and that no unfolding intermediates were present. However, for the mutant, this phase is less sensitive to urea ($m_u = 405.9$ J/mol per M urea) than the corresponding phase of the wild type ($m_u = 1129.7$ J/mol per M urea) [18]. These low m_u values indicate that the transition state for the slow phase of both wild-type and P56G mutant relates closely to the solvent-accessible surface area of the native state [18]. The unfolding rates of thioredoxin were also increased for the *cis*-proline mutant [8].

Conclusion

The findings from this and other studies indicate the significance of the role played by the topologically conserved *cis*-proline in the catalytic activity and conformational stability of not only the GSTs, but also other members of the thioredoxin-like superfamily that possess the *cis*-proline. These proteins have short loop sequences connecting α-helix 2 to β-strand 3, with the C-terminus of the loop requiring the sharp bend offered by a *cis*-proline to connect to β-strand 3. Those proteins containing a thioredoxin-like domain but no *cis*-proline topologically equivalent to Pro-56 in hGST A1-1 belong mainly to the glutathione peroxidase-like family (see http://scop.mrc-lmb.cam.ac.uk/scop/data/scop.b.d.fe.b.html). They typically have a longer loop sequence connecting α-helix 2 to β-strand 3, and the conformation of the loop does not require a sharp bend when it connects to β-strand 3.

This work was supported by the University of the Witwatersrand, the South African National Research Foundation, and the Wellcome Trust (grant number 060799).

REFERENCES

1 Sheehan, D., Meade, G., Foley, V. M. and Dowd, C. A. (2001) Structure, function and evolution of glutathione transferases: implications for classification of non-mammalian members of an ancient enzyme superfamily. Biochem. J. **360**, 1–16

2 Xia, B., Vlamis-Gardikas, A., Holmgren, A., Wright, P. E. and Dyson, H. J. (2001) Solution structure of *Escherichia coli* glutaredoxin-2 shows similarity to mammalian glutathione-S-transferases. J. Mol. Biol. **310**, 907–918

3 Bousset, L., Belrhali, H., Melki, R. and Morera, S. (2001) Crystal structures of the yeast prion Ure2p functional region in complex with glutathione and related compounds. Biochemistry **40**, 13564–73
4 Harrop, S. J., DeMaere, M. Z., Fairlie, W. D., Reztsova, T., Valenzuela, S. M., Mazzanti, M., Tonini, R., Qiu, M. R., Jankova, L., Warton, K. et al. (2001) Crystal structure of a soluble form of the intracellular chloride ion channel CLIC1 (NCC27) at 1.4-A resolution. J. Biol. Chem. **276**, 44993–45000
5 Wallace, L. A. and Dirr, H. W. (1999) Folding and assembly of dimeric human glutathione transferase A1-1. Biochemistry **38**, 16686–16694
6 Widersten, M. and Mannervik, B. (1995) Glutathione transferases with novel active sites isolated by phage display from a library of random mutants. J. Mol. Biol. **250**, 115–122
7 Dirr, H., Reinemer, P. and Huber, R. (1994) X-ray crystal structures of cytosolic glutathione S-transferases. Implications for protein architecture, substrate recognition and catalytic function. Eur. J. Biochem. **220**, 645–661
8 Kelley, R. F. and Richards, F. M. (1987) Replacement of proline-76 with alanine eliminates the slowest kinetic phase in thioredoxin folding. Biochemistry **26**, 6765–6774
9 Charbonnier, J. B., Belin, P., Moutiez, M., Stura, E. A. and Quemeneur, E. (1999) On the role of the *cis*-proline residue in the active site of DsbA. Protein Sci. **8**, 96–105
10 Wang, R. W., Newton, D. J., Johnson, A. R., Pickett, C. B. and Lu, A. Y. (1993) Site-directed mutagenesis of glutathione S-transferase YaYa. Mapping the glutathione-binding site. J. Biol. Chem. **268**, 23981–23985
11 Allocati, N., Casalone, E., Masulli, M., Caccarelli, I., Carletti, E., Parker, M. W. and Di Ilio, C. (1999) Functional analysis of the evolutionary conserved proline 53 residue in *Proteus mirabilis* glutathione transferase B1-1. FEBS Lett. **445**, 347–350
12 Stenberg, G., Björnestedt, R. and Mannervik, B. (1992) Heterologous expression of recombinant human glutathione transferase A1-1 from a hepatoma cell line. Protein Exp. Purif. **3**, 80–84
13 Sayed, Y., Wallace, L. A. and Dirr, H. W. (2000) The hydrophobic lock-and-key intersubunit motif of glutathione transferase A1-1: implications for catalysis, ligandin function and stability. FEBS Lett. **465**, 169–172
14 Laemmli, U. K. (1970) Cleavage of structural proteins during the assembly of the head of bacteriophage T4. Nature (London) **227**, 680–685
15 Perkins, S. J. (1986) Protein volumes and hydration effects. The calculations of partial specific volumes, neutron scattering matchpoints and 280-nm absorption coefficients for proteins and glycoproteins from amino acid sequences. Eur. J. Biochem. **157**, 169–180
16 Habig, W. H. and Jakoby, W. B. (1981) Assays for differentiation of glutathione S-transferases. Methods Enzymol. **77**, 398–405
17 Dirr, H. W. and Reinemer, P. (1991) Equilibrium unfolding of class pi glutathione S-transferase. Biochem. Biophys. Res. Commun. **180**, 294–300
18 Wallace, L. A., Sluis-Cremer, N. and Dirr, H. W. (1998) Equilibrium and kinetic unfolding properties of dimeric human glutathione transferase A1-1. Biochemistry **37**, 5320–5328
19 Pace, C. N., Shirley, B. A. and Thomson, J. A. (1989) Measuring the conformational stability of a protein. In Protein Structure: a Practical Approach, 2nd edn (Creighton, T. E., ed.), pp. 311–330, IRL Press/Oxford University Press, Oxford
20 Stenberg, G., Abdalla, A. M. and Mannervik, B. (2000) Tyrosine 50 at the subunit interface of dimeric human glutathione transferase P1-1 is a structural key residue for modulating protein stability and catalytic function. Biochem. Biophys. Res. Commun. **271**, 59–63
21 Hornby, J. A., Luo, J. K., Stevens, J. M., Wallace, L. A., Kaplan, W., Armstrong, R. N. and Dirr, H. W. (2000) Equilibrium folding of dimeric class mu glutathione transferases involves a stable monomeric intermediate. Biochemistry **39**, 12336–12344
22 Wallace, L. A., Blatch, G. L. and Dirr, H. W. (1998) A topologically conserved aliphatic residue in alpha-helix 6 stabilizes the hydrophobic core in domain II of glutathione transferases and is a structural determinant for the unfolding pathway. Biochem. J. **336**, 413–418
23 Sinning, I., Kleywegt, G. J., Cowan, S. W., Reinemer, P., Dirr, H. W., Huber, R., Gilliland, G. L., Armstrong, R. N., Ji, X., Board, P. G. et al. (1993) Structure determination and refinement of human Alpha class glutathione transferase A1-1, and a comparison with the Mu and Pi class enzymes. J. Mol. Biol. **232**, 192–212
24 Stenberg, G., Board, P. G. and Mannervik, B. (1991) Mutation of an evolutionarily conserved tyrosine residue in the active site of a human class Alpha glutathione transferase. FEBS Lett. **293**, 153–155
25 Bjornestedt, R., Stenberg, G., Widersten, M., Board, P. G., Sinning, I., Jones, T. A. and Mannervik, B. (1995) Functional significance of arginine 15 in the active site of human class alpha glutathione transferase A1-1. J. Mol. Biol. **247**, 765–773
26 Eklund, H., Cambillau, C., Sjoberg, B. M., Holmgren, A., Jornvall, H., Hoog, J. O. and Branden, C. I. (1984) Conformational and functional similarities between glutaredoxin and thioredoxins. EMBO J. **3**, 1443–1449
27 Soulages, J. L. (1998) Chemical denaturation: potential impact of undetected intermediates in the free energy of unfolding and m-values obtained from a two-state assumption. Biophys. J. **75**, 484–492
28 Wallace, L. A., Burke, J. and Dirr, H. W. (2000) Domain-domain interface packing at conserved Trp-20 in class alpha glutathione transferase impacts on protein stability. Biochim. Biophys. Acta **1478**, 325–332
29 Tasayco, M. L., Fuchs, J., Yang, X. M., Dyalram, D. and Georgescu, R. E. (2000) Interaction between two discontiguous chain segments from the beta-sheet of *Escherichia coli* thioredoxin suggests an initiation site for folding. Biochemistry **39**, 10613–10618
30 Dragani, B., Iannarelli, V., Allocati, N., Masulli, M., Cicconetti, M. and Aceto, A. (1998) Irreversible thermal denaturation of glutathione transferase P1-1. Evidence for varying structural stability of different domains. Int. J. Biochem. Cell Biol. **30**, 155–163
31 Kraulis, J. P. (1991) MOLSCRIPT: a program to produce both detailed and schematic plots of protein structures. J. Appl. Crystallogr. **24**, 946–950

Received 12 November 2002/29 January 2003; accepted 7 February 2003
Published as BJ Immediate Publication 7 February 2003, DOI 10.1042/BJ20021765